Triangle defect states of hexagonal boron nitride atomic layer: Density functional theory calculations

Li-Chang Yin,[1,2,*] Hui-Ming Cheng,[2] and Riichiro Saito[1]
[1]*Department of Physics, Tohoku University, Sendai 980-8578, Japan*
[2]*Shenyang National Laboratory for Materials Science, Institute of Metal Research, Chinese Academy of Science, 72 Wenhua Road, Shenyang 110016, China*

(Received 2 September 2009; revised manuscript received 25 March 2010; published 15 April 2010)

Triangle defect states of hexagonal boron nitride (h-BN) atomic layer were studied by a density functional theory calculation. N(B) triangle defect states of h-BN atomic layer with N(B) edge atoms have acceptor (donor) levels. A cohesive energy calculation indicates that the h-BN atomic layer with N triangle defects is more or less stable, respectively, than that with B triangle defects when it is negatively or positively charged, which is consistent with the recent experimental observation of N triangle defects in h-BN atomic layer. Charge population analysis shows that the edge N(B) atoms surrounding the N(B) triangle defect are negatively (positively) charged. Such a charged triangle defects in h-BN may serve as a potential nanolens for electron-beam focusing.

DOI: 10.1103/PhysRevB.81.153407 PACS number(s): 71.15.Nc, 71.55.Eq, 73.22.−f, 61.72.jd

A single carbon atomic layer structure named graphene which exhibits unique properties, such as high carrier mobility, ambipolar effect, the Klein tunneling, quantum hall effect, etc., has been expected to offer novel applications in various fields.[1] As a result, other two-dimensional (2D) atomic layers are also attracting significant interest owing to their exceptional properties.[2] Among them, a hexagonal boron nitride (h-BN) sheet which is the group III-V isoelectronic analog of graphene has also been synthesized.[3–5] A single atomic layer of h-BN is a wide-gap semiconductor like three-dimensional (3D) h-BN (Refs. 6 and 7) and is a promising material in optoelectronics.[8] Moreover, one-dimensional h-BN nanoribbons with zigzag edges are predicted to show metallic, semiconducting, and half-metallic transitions by applying an external electric field.[9] Recently, Jin *et al.*[10] have successfully fabricated a free-standing single layer of h-BN and observed atomic defects with triangle shape in the h-BN. The dominating zigzag-type edge atoms along the triangle defects are proved to be nitrogen atoms. They suggested that boron vacancies are more energetically stable. However, previous theoretical and experimental[11–14] studies indicate that the formation energy of a boron monovacancy is larger than that of a nitrogen monovacancy, thus the formation of nitrogen monovacancy is preferable, which is opposite to the experimental results of Jin *et al.*[10] Usually, the kinetic energy of the electrons in the transmission electron microscopy (TEM) system quickly decays (in 10–100 fs) in solid by electron-electron interaction, which is much faster than the structural change (at least more than 1 ps). In fact, the energy (120 keV) of the electron beam employed in the experiment of the TEM measurements[10] is much larger than the threshold beam energies for knock on of both B (74 keV) and N (84 keV) (Ref. 15) atoms. However, as discussed in Ref. 10, if the knock-on effect is important, the selective formation of the boron vacancies would not occur but both nitrogen and boron vacancies should appear at the same time. Considering the electron-rich environment in the TEM, the effect of charge (not kinetic energy) should be important to explain the selective formation of boron vacancies,[10] which is the motivation of the present work.

In h-BN atomic layer, N(B) atoms are negatively (positively) charged because of ionic character of the crystal and the formation energy of N(B) edge atoms should depend on the ionicity. It is the reason why B atoms are preferentially removed by electron irradiation and form N-edged triangle defects.[10] A 3D h-BN crystal is a wide-gap semiconductor with an energy gap of 4.02 ± 0.01 eV (Ref. 16) in which the valence (conduction) energy band consists of mainly N(B) atoms. If we naively consider that B wave function in the conduction band does not contribute much to the B-N covalent bond compared with N wave function in the valence band, B atom might have a smaller dissociation energy than N atom. However, as was shown in the previous calculation for a point defect,[11] the situation is opposite to this consideration, which means that N atoms can be more easily dissociated.

An important fact to consider is that the B(N) edge states[17] appear around B(N) zigzag edges of a B(N) triangle defect. Hereafter, the triangle defects with B(N) zigzag edges, which are formed by removing more N(B) atoms than B(N) atoms from h-BN, are called B(N) triangle defects. The B(N) edge states form donor (acceptor) states near conduction (valence) energy bands, which show opposite behavior for B(N) atoms in Si. Another critical issue is that how many electrons can donate (accept) from the B(N) edge states, which should be sensitive to the dissociation energy.

In this Brief Report, we present a detailed, density functional theory (DFT) calculation of atomic and electronic structures of h-BN atomic layer with different sizes of N and B triangle defects. Negatively charged N triangle defects well reproduce the experimental condition of Jin *et al.*, which is an electron enriched environment induced by electron irradiation. The stability of neutral or charged N(B) triangle defects is investigated by cohesive energy calculation. We found that N(B) triangle defects prefer to be negatively (positively) charged. Such an oppositely charged tendency for N and B triangle defects is well explained by density-of-states (DOS) calculation. Further, we found that N(B) triangle defect shows a negatively (positively) charged triangle, whose charge can be modified by changing the Fermi energy.

 ©2010 The American Physical Society

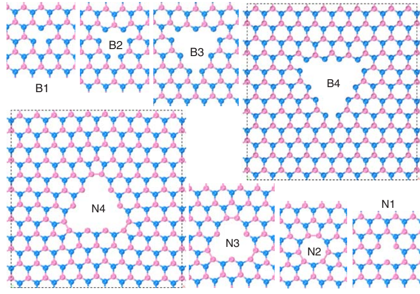

FIG. 1. (Color online) Schematic representation of full relaxed B*n* and N*n* triangle defects ($n=1,\ldots,4$) with n B (blue) and n N (red) edge atoms for each edge of the triangle. A N-N bond and a pentagon ring form at each vertex of N triangle defects for N2, N3, and N4 defects. The dashed rectangles for B4 and N4 are supercells that are used in the present calculations for all triangle defects.

Using the nanosized potential, we propose a possible application for nanolens for electron-beam focusing.

The DFT calculations were performed by using the projector-augmented wave method[18] and the Perdew-Burke-Ernzerhof[19] functional as implemented in VASP code.[20] We use a single k point (Γ point) and plane waves with energies up to 440 eV, which ensures the convergence precision of total energy within 1 meV per atom. The geometry structure was fully optimized by minimizing the Hellmann-Feynman force smaller than 0.03 eV/Å without any symmetric constraint. A large 2D periodic supercell with a large vacuum space (15 Å) in z direction including 240 atoms (120 B and 120 N atoms) is constructed to represent the 2D *h*-BN atomic layer as shown in Fig. 1. For 2D *h*-BN atomic layer without a defect, the optimized B-N bond length is 1.444 Å, which is consistent with the experimental value (1.44 ± 0.1 Å).[10] The equilibrium cohesive energy is calculated to be 7.072 eV per atom, which is consistent with other DFT results of 3D *h*-BN by using the same exchange-correlation functional, ranged from 7.071 to 7.076 eV per atom depending on different stackings.[21] 2D *h*-BN is a semiconductor with a calculated band gap $E_G=4.42$ eV, which is 5% smaller than a recent theoretical value, 4.64 eV.[7]

In this work, B and N triangle defects with four different sizes are considered (Fig. 1). Here, B*n* ($n=1$, 2, 3, and 4) represents four B triangle defects with (a) 1, (b) 2, (c) 3, and (d) 4 edge B atoms at each triangle edge, respectively, and N*n* ($n=1$, 2, 3, and 4) denotes four N triangle defects. The fully relaxed structures of the *h*-BN atomic layer with B and N triangle defects are presented in Fig. 1. As can be seen in Fig. 1, compared with pristine *h*-BN atomic layer, no noticeable structure change can be observed for monovacancy defects B1 and N1. For B triangle defects, i.e., B2, B3, and B4, a small structure distortion at triangle vertex appears, which results in three pairs of two-coordinated B atoms at three vertexes of the B triangle defects. The typical B-N bond lengths for two-coordinated B edge atoms in B triangle defects are calculated to be 1.46 Å (B1), 1.45 and 1.47 Å (B2), 1.45, 1.47, and 1.44 Å (B3), and 1.46, 1.48, 1.49, and 1.44 Å (B4). In contrast to the B triangles, N2, N3, and N4 show distinct structure distortion. In fact, an N-N bond and a pentagonal ring form at each vertex of N triangle defects (N2, N3, and N4), which results in three coordinations for all vertex N atoms. In the case of N1, strong Coulomb repulsive interaction between three edge N atoms prevents the formation of N-N bond and results in a larger atomic distance 2.59 Å between the edge N atoms than that (2.49 Å) of pristine *h*-BN atomic layer. The calculated N-N bond lengths decrease with increasing the size of N triangle defects, which are 1.55, 1.49, and 1.47 Å for N2, N3, and N4, respectively, and are slightly larger than but comparable with that (1.35 Å) of N-N single bond in the cubic gauche nitrogen (*cg*-N).[22] Such a N-N bonding can be further confirmed by local DOS calculation and the charge population analysis. The edge N atoms around the triangular defects in *h*-BN are negatively charged, which induces the Coulomb repulsive between two N atoms, resulting in longer N-N bonding length. The N-B bond lengths for two-coordinated N edge atoms in N triangle defects are 1.40 Å (N1), 1.41 Å (N3), and 1.39 and 1.42 Å (N4), respectively. The formation of three pentagons at three vertexes should be very helpful to assign the edge atom along the zigzag edges for N triangle defects by scanning tunneling microscope. Meanwhile, the formation of the N-N bonds at three vertexes induces the increase in atomic distance between other edge N atoms, which are calculated to be 2.74, 2.67, and 2.58–2.63 Å for N2, N3, and N4, respectively, well reproducing the measured distances ranging from 2.63 to 2.72 Å, by exit-wave reconstruction of the high-resolution transmission electron microscopy image.[10] We noticed that the Jahn-Teller effect and out-of-plane relaxation of edge C atom were observed in a defective graphene with triangle vacancies.[23] However, these effects could not be observed for *h*-BN. As shown in Fig. 1, all triangular defects consist of zigzag edges, which gives rise to localized edge states.[17] The Coulomb interaction ($\sim$2 eV) (Ref. 6) between two electrons in such localized edge states for *h*-BN is larger than a typical level splitting (around the order of phonon energy, $\sim$0.1 eV). The Jahn-Teller effect does not occur for the degenerate states, which is confirmed by the full optimization calculations. However, in the case of graphene, since the screening effect by the other electrons is strong due to a metallic character of graphene, the Coulomb interaction should be suppressed significantly, thus the Jahn-Teller effect or out-of-plane distortion is expected for graphene with triangular vacancy defects.[23]

Since the experimental observation of N triangle defects in *h*-BN is related to electron irradiation of high-energy (120 keV) electron beam,[10] different charged states may occur simultaneously in which electrons are not in the thermal equilibrium state. In this case, the conventional method[23,24] to evaluate the relative stability of defects in *h*-BN by calculating the formation energy as a function of electron chemical potential is not suitable. Due to the Fermi-level pinning originated from the in-gap defect state for *h*-BN with triangular defect, the electron chemical potential changes discontinuously by applying a gate voltage while the charge changes continuously. We do not consider the N-rich and B-rich environments in present work because free B(N) atoms or clusters could not exist around the defective area under a high-energy (120 keV) electron beam, which is much higher than the threshold knock-on energy for both B (74 keV) and N (84 keV) atoms. Thus, it is more reasonable to

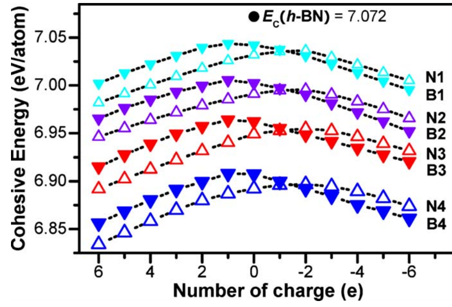

FIG. 2. (Color online) Cohesive energies E_c as a function of number of charge in the supercell for *h*-BN atomic layer with N (open △) and B (solid ▽) triangle defects. The E_c of neutral 2D *h*-BN is indicated by a black dot.

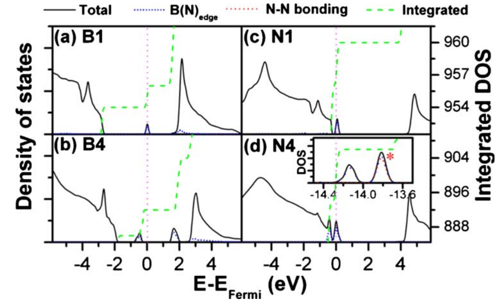

FIG. 3. (Color online) Density of states plots as a function of energy for (a) B1, (b) B4, (c) N1, and (d) N4 triangle defects. Here, the total and local DOS are plotted for one *k* point sampling with 0.2 eV broadening. The N-N bonding state of N4 is shown in the upper right inset of Fig. 3(d) and marked by a red asterisk. Black solid lines are total DOS. Blue short dashed lines are local DOS of B(N) edge atoms. Red short dot line indicates the N-N bonding state. Green dashed lines denote integrated DOS and the red dot line denotes the Fermi energy.

choose the cohesive energy calculation as a function of charge to evaluate the stability of charged defects. In order to reproduce the electron-rich environment, we have calculated the cohesive energies E_c for B and N triangle defects as a function of additional charge from $+6e$ to $-6e$ ($e>0$) per supercell ($1e$ per supercell corresponding to $1.6\times10^{13}e/\text{cm}^2$), as shown in Fig. 2, by using the following expression:

$$E_c = (n_B E[\text{B}] + n_N E[\text{N}] - E[\text{BN}])/(n_B + n_N), \qquad (1)$$

where $E[\text{B}](E[\text{N}])$ is the energy of isolated B(N) atom and $E[\text{BN}]$ is the total energy of *h*-BN atomic layer with triangle defects, $n_B(n_N)$ is the number of B(N) atoms in the *h*-BN supercell. It should be noted that a larger E_c means more stable structure. In the neutral case, the E_c decreases with increasing the triangle size for B(N) triangle defects and is smaller than that of 2D *h*-BN, and the E_c of B triangle defects is always larger than that of N triangle defects, which is consistent with earlier theoretical and experimental results.[11–13] For the monovacancy N1, strong Coulomb repulsive interaction between negatively charged edge N atoms decreases E_c. For large N triangle defects, the formation of N-N bond makes large structure distortion and results in pentagon formation, which makes the N triangle defects less stable. On the other hand, all B triangle defects with four different sizes show small structure deformation, which contributes to a larger stability than that of N triangle defects. Thus, the Bn is more stable than Nn for the neutral case.

As for charged triangle defects, the calculated E_c depends on the sign and number of charges as shown in Fig. 2. For B triangle defects, the E_c has a maximum at $e=+1$ and decreases with increasing the number of positive or negative charge. However, the E_c of N triangle defects reaches the maximum around $e=-2$. Thus, E_c's cross at $e=-1$ for B triangle and N triangle defects with four different sizes. Thus, we obtain larger E_c of N triangle defects for negative charged 2D *h*-BN for $e\leq-2$. This means that the *h*-BN atomic layer with N triangle defects is more (less) stable than that with B triangle defects in case of negatively (positively) charged environment.

We expect an electron enriched environment by electron irradiation in the transmission electron microscope measurement. This is the reason why they observe only N triangle defect in the experiment,[10] which is consistent with the present E_c calculation. In order to confirm this, we next estimate how many electrons a N(B) triangle defect can accept (donate).

In Fig. 3, the DOS and integrated DOS are plotted for the *h*-BN atomic layer for two different sizes of B and N triangle defects. We present the DOS plots only for two B and N triangle defects because of the similarity of the other two different sizes. As we can see from Fig. 3, the DOS plots show an edge states (or defect states) in the energy gap. In the cases of B triangle defects, a partially occupied states appear around the gap center for B1 [Fig. 3(a)] and an unoccupied states appear about 0.31 eV below the bottom of the conduction band for B4 [Fig. 3(b)], depending on removing odd or even number of atoms, respectively. These states mainly consist of B zigzag edge[17] states by local DOS (blue short dashed lines in Fig. 3) analysis. We call these triangle defect states deep and shallow donor states caused by removing N atoms. In Figs. 3(c) and 3(d), a partially occupied DOS peak always appears close to the valence-band N triangle defects, which consists of N zigzag edge states by local DOS analysis. We simply call them acceptor states. This situation with donor (B) and acceptor (N) states in *h*-BN atomic layer with triangle defects is opposite to that with impurity states of B and N atoms in Si. From the integrated DOS, we found that the deep donor states of B1 can accommodate only two electrons and have already been half occupied by one electron. Thus, the Fermi level of B1 shifts down to the valence band by removing this occupying electron. For B4, since the shallow donor states lie close to the conduction band, which require more energy for additional electrons to occupy. This is the reason for the smaller E_c of negatively charged B triangle defects. Further, the partially occupied acceptor states for N triangle defects lie close to the valence band can accommodate additional electrons with small energy cost, which can explain the maximum E_c at $e=-2$ for N triangle defects. Integrated DOS show that the acceptor states can accept 3–4 electrons. Moreover, as shown in the inset of Fig. 3(d), the N-N bonding state appear around -13.8 eV lower than the Fermi level for N2, N3, and N4, which approves the formation of N-N bonds.

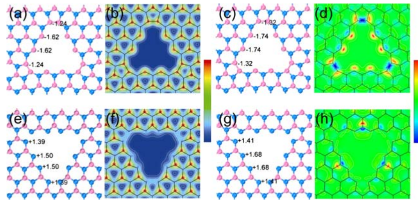

FIG. 4. (Color online) Charge population and charge density of the *h*-BN atomic layer with triangle defects. (a) charge population of N4, (b) total charge density of N4, (c) charge population of negatively charged N4 with 2 electrons, (d) difference charge density of N4, (e) charge population of B4, (f) total charge density of B4, (g) charge population of positively charged B4 with 2 electrons, and (h) difference charge density of B4.

It is important to discuss charge distribution around the N and B triangle defects. The charge population was calculated by using Bader charge analysis.[25,26] Based on the charge population analysis, B(N) atom of pristine *h*-BN is positively (negatively) charged with $+0.67e$ ($-0.67e$), which verifies the ionic covalent character of a B-N bond. In the case of N monovacancy (N1), each edge N atom is negatively charged with $-1.59e$ and bonds with two B atoms, which means the edge N atom has $-0.25e$ $[-1.59e+2\times(+0.67e)=-0.25e]$ negative charge. This net negative charge ($-0.25e$) induces a strong Coulomb repulsive interaction among three edge N atoms. In Fig. 4, we plot the charge population, total charge densities, and difference charge densities for N4 and B4 defects. Here, the difference charge density is given by subtracting the total charge density of neutral triangle defects from that of charged triangle defects. As we can see from Fig. 4(b), large charge density at the triangle vertex indicates the N-N bonding in N4. The total charge-density plot shows an electron enriched region surrounding the edges of N triangle defect, which means that the N triangle defect is negatively charged. Such a negatively charged N triangle defect can be proved by charge population analysis [Fig. 4(a)], and those two-coordinated N atoms appear to be negatively charged with 1.62 electrons per atom, and three pairs of N atoms locating at the triangle vertexes are also negatively charged with 1.24 electrons per atom after forming N-N bond. When the N4 is negatively charged ($-2e$), 1.2 electrons are localized at the zigzag edge N atoms [Fig. 4(c)] which are calculated to be $-1.74e$ and $-1.32e$ electrons per atom for six edge N atoms and other six N atoms forming three N-N bonds, respectively. The difference charge-density plot [Fig. 4(d)] clearly shows that additional electrons are located at edges. On the other hand, as shown in Figs. 4(f) and 4(g), the electron-deficient area surrounding the B triangle edge indicates a positively charged ($+1.39e$,$+1.50e$) edge in the B triangle defect. When the B4 is positively charged by two electrons ($+2e$), all zigzag edge B atoms are more positively charged [Fig. 4(g)] with $+1.41e$ and $+1.68e$ electrons per atom for six zigzag edge B atoms and other six vertical B atoms, respectively, which means that $+1.2e$ of the $+2e$ is localized at the edges [Fig. 4(g)]. If we control the Fermi energy by a gate electrode, we can make B triangle defects by electron irradiation as well. An important result is that the charge at the edge atoms can be controlled by the gate electrode. Thus, a nanometer sized vacancy can be used for nanolens for electron-beam focusing by combining N and B triangle defects in which the focus length can be controlled by the gate voltage, which will be reported elsewhere.

In summary, DFT calculation was performed to study the atomic and electronic structures of a *h*-BN atomic layer with B triangle and N triangle defects. For the N triangle defects, the formation of N-N bond in the triangle vertex results in the formation of pentagon, which should be checked by scanning tunneling microscopy. Cohesive energy calculation indicates that the negatively charged *h*-BN with N triangle defects is more stable than that with B triangle defects. The triangle defect states of the B(N) triangle defects lie close to the conduction (valence) band, forming the donor (acceptor) levels. Such triangle defect states are not fully occupied and can accommodate additional electrons with small energy cost, which is relevant to the stability of triangle defects. Our DFT calculations can well explain the recently observed N triangle defects in a free-standing *h*-BN. Moreover, the ionicity of B and N triangle defects can be controlled by changing the Fermi energy, respectively, which may be used as future nanolens for electron-beam focusing with high resolution.

Li-Chang Yin and R. Saito acknowledge MEXT under Grant No. 20241023. We also acknowledge the support from Supercomputing Center of CAS.

*lcyin@imr.ac.cn

[1] A. K. Geim and K. S. Novoselov, Nature Mater. **6**, 183 (2007).
[2] K. S. Novoselov *et al.*, Proc. Natl. Acad. Sci. U.S.A. **102**, 10451 (2005).
[3] D. Pacilé *et al.*Appl. Phys. Lett. **92**, 133107 (2008).
[4] W. D. Han *et al.*, Appl. Phys. Lett. **93**, 223103 (2008).
[5] J. C. Meyer *et al.*, Nano Lett. **9**, 2683 (2009).
[6] X. Blase *et al.*, Phys. Rev. B **51**, 6868 (1995).
[7] M. Topsakal *et al.*, Phys. Rev. B **79**, 115442 (2009).
[8] K. Watanabe *et al.*, Nature Mater. **3**, 404 (2004).
[9] V. Barone and J. E. Peralta, Nano Lett. **8**, 2210 (2008).
[10] C. Jin *et al.*, Phys. Rev. Lett. **102**, 195505 (2009).
[11] S. Azevedo *et al.*, Nanotechnology **18**, 495707 (2007).
[12] I. Jiménez *et al.*, Appl. Phys. Lett. **68**, 2816 (1996).
[13] I. Jiménez *et al.*, Phys. Rev. B **55**, 12025 (1997).
[14] W. Orellana and H. Chacham, Phys. Rev. B **63**, 125205 (2001).
[15] A. Zobelli *et al.*, Phys. Rev. B **75**, 245402 (2007).
[16] V. L. Solozhenko *et al.*, J. Phys. Chem. Solids **62**, 1331 (2001).
[17] F. Zheng *et al.*, J. Phys. Soc. Jpn. **78**, 074713 (2009).
[18] P. E. Blöchl, Phys. Rev. B **50**, 17953 (1994).
[19] J. P. Perdew *et al.*, Phys. Rev. Lett. **77**, 3865 (1996).
[20] G. Kresse and J. Furthmüller, Phys. Rev. B **54**, 11169 (1996).
[21] N. Ooi *et al.*, Modell. Simul. Mater. Sci. Eng. **14**, 515 (2006).
[22] M. I. Eremets *et al.*, Nature Mater. **3**, 558 (2004).
[23] A. A. El-Barbary *et al.*, Phys. Rev. B **68**, 144107 (2003).
[24] S. Okada, Phys. Rev. B **80**, 161404 (2009).
[25] R. Bader, *Atoms in Molecules: A Quantum Theory* (Oxford University Press, New York, 1990).
[26] G. Henkelman *et al.*, Comput. Mater. Sci. **36**, 354 (2006).